International Commission on Illumination
Commission Internationale de l'Eclairage
Internationale Beleuchtungskommission

PO160

OPTIMIZATION OF TUNNEL LIGHTING CONTROL BY RE-AIMING OF THE EXTERNAL L20 LUMINANCE METER

Constantinos Bouroussis et al.

DOI 10.25039/x46.2019.PO160

from

CIE x046:2019

Proceedings
of the
29th CIE SESSION
Washington D.C., USA, June 14 – 22, 2019

(DOI 10.25039/x46.2019)

The paper has been presented at the 29th CIE Session, Washington D.C., USA, June 14-22, 2019. It has not been peer-reviewed by CIE.

CIE Central Bureau
Babenbergerstrasse 9
A-1010 Vienna
Austria
Tel.: +43 1 714 3187
e-mail: ciecb@cie.co.at
www.cie.co.at

OPTIMIZATION OF TUNNEL LIGHTING CONTROL BY RE-AIMING OF THE EXTERNAL L20 LUMINANCE METER

Bouroussis, C.A.[1], Nikolaou, D.T.[1], Topalis, F.V.[1]
[1] National Technical University of Athens, Lighting Laboratory, Athens, GREECE
bouroussis@gmail.com

DOI 10.25039/x46.2019.PO160

Abstract

The lateral position of the L_{20} meter in tunnels introduces disparities between the corresponding L_{20} field of view (FOV) as seen by the driver and as captured by the meter. This paper presents a study on the effect of the variance of the components of L_{20} FOV on the portal luminance at various orientations. It includes thousands of calculations of alternative L_{20} FOV and a sensitivity analysis on the variation of annual energy consumption. The results indicate that the differences in the field of view, may trigger a rather different lighting installation operational profile than the one anticipated from the lighting design which would be a compromise in both safety and energy consumption. The paper proposes a method of re-aiming of the external L_{20} meters in tunnels in order to optimise the operation of the lighting control system concerning traffic safety and the annual energy consumption.

Keywords: Tunnel Lighting, Lighting Controls, L20 meter, Optimization, Energy consumption, Relux Tunnel, Matlab

1 Introduction

The tunnel lighting design is performed with the use of CIE 88 technical report (CIE 2004), (CIE 2010), as well as other national and / or international standards. The design of the lighting during daytime is particularly critical because of the human visual system restraints. The typical observer (driver) outside the tunnel cannot simultaneously perceive details on the road under lighting levels existing in a highly illuminated exterior environment and a relatively dark interior. The entrance lighting aims to reduce the "black hole" effect at the entrance of a tunnel and enable the driver's vision to easily adapt to the lighting inside the tunnel. Due to the driver's safety and visibility requirements, as well as reasonable energy consumption profiling requirements, the day time lighting follows the exterior luminance changes.

The common practice among the tunnel lighting guides, is that the exterior luminance is measured through an external luminance meter. The meter comprises either a single photo detector or an imaging sensor (ILMDs). The role of that instrument is to measure the luminance of the tunnel portal on a particular conical field of view (FOV). The geometry of the FOV depends on the used calculation method (e.g. L_{20} or L_{seq} method) as described in CIE 88.

The adaptation of the lighting installation is based on the exterior luminance which is a product of various components. According to CIE 88, the L_{20} (or L_{seq}) is defined as the luminance that is measured or calculated from the position of the typical observer at the safe stopping distance in front of the tunnel portal. This luminance is composed of the luminance values of the various elements that are included into the FOV, namely, sky, road, rocks, buildings, snow, meadows. A key factor is also the orientation of the tunnel and the geographic location of it. The percentile mixture of the sub elements inside the field of view determines the final exterior luminance level. Therefore, each tunnel has its variation of the external luminance and a mixture of elements that build up the final luminance level. This luminance level is considered as the nominal L_{20} in this study.

Regardless of the calculation method of the exterior luminance (L_{20} or L_{seq}), the calculation takes place using a FOV from a location that is impossible to be considered in real installation conditions as a possible installation position of the luminance meter. If a full replication of the exact mixture of the elements of the field of view of the typical observer takes place, the external

luminance meter will be installed at this exact position, and therefore, the field of view and the luminance measurement will always be correct.

In real practice, a typical installation position of the luminance meters would be on the side of the road, adjacent to the traffic lanes, at a height 3-5m higher than the observer's height and in some cases at a distance different than the stopping distance due to manufacturing restrictions or other reasons, facing the centre of the tunnel portal.

This results in a different composition in the field of view of the meter compared to a luminance meter that theoretically should be located at the typical observer position, in the middle of the road. Moreover, it could be also a common problem that several obstacles may block part of the field of view of the meter, resulting in a significantly different measured luminance compared to the anticipated designed one. This luminance level is considered as the meter's L_{20} in this study.

Many recent studies consider the energy consumption or the external luminance of a tunnel, e.g. (Bouroussis 2011), (Lorphevre 2016), (Lopez 2017), but there is no recent work on the issues produced due to the lateral position of the external luminance meters.

The potential differences of the mixture of elements in the camera's field of view, due to its location, result to unreliable luminance measurements and consequently to early or late triggering of certain luminance levels inside the tunnel, resulting to an over-illuminated or an under-illuminated tunnel in the corresponding period. This affects both the safety of the tunnel (over -illumination or under-illumination) as well as the energy consumption of the tunnel.

This paper aims to calculate and evaluate the possible differences in luminance measurements as described above, through the correct re-aiming of the exterior luminance meters. The purpose of this action is the increase of the accuracy between the theoretical lighting design and the actual installation, which is a matter of road safety, as well as the optimization of the energy profile usage of the tunnel lighting system. The latter results in energy savings or more expenditures depending on the orientation of the tunnel and the nature of the differences in the perceived field of view.

2 The concept of the L_{20} meter re-aiming

This paper deals exclusively with the calculation method of L_{20} as described in CIE 88. As thoroughly described above, the lateral positioning of the external luminance meter influences the field of view of the instrument that is most likely different compared to the FOV of the typical observer. Therefore, this work focuses on the investigation of the effect of the variation of the FOV with respect to the expected difference in luminance measurement and the behaviour of the tunnel lighting control system.

According to CIE 88, the L_{20} is calculated using the equations (1) and (2).

$$L_{20} = \gamma L_c + \rho L_r + L_e \varepsilon + L_{th} \tau \quad (1)$$

where:

L_c: luminance of the sky — γ = % of sky in the 20° FOV

L_r: luminance of the road — ρ = % road

L_e: luminance of the surroundings — ε = % of surroundings

L_{th}: luminance of the threshold zone — τ = % of tunnel portal

and

$$\gamma + \rho + \varepsilon + \tau = 1 \text{ or } 100\ \% \quad (2)$$

The lateral position of the L_{20} meter is expected to introduce potential differences between the luminance from the observer's position and the meter reading. Figure 1 shows the basic concept of the proposed re-aiming of the external luminance meter. The left graph illustrates an example of the L_{20} FOV as seen from the driver's position from the stopping distance. The middle graph

illustrates the potential FOV of the L_{20} meter that is placed in a lateral position at the stopping distance (potentially also closer or further away) aiming at the portal centre. The graph on the right illustrates the optimized L_{20} FOV of the meter where the aiming point is different from the tunnel portal. This new aiming point will be determined after the optimum selection of the FOV. The optimized FOV may be exact the same as the one of the typical driver or the one that produces the same luminance variation to the typical driver. In these illustrations, the subscripts n for nominal, m for meter and o for optimal are used for the L_{20} components (sky, road, surrounding and portal) accordingly.

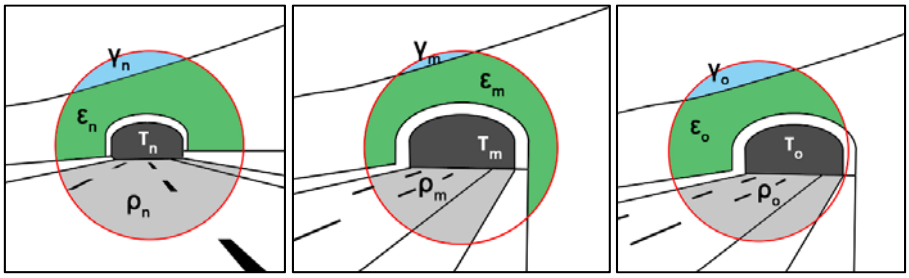

Figure 1 – The concept of L_{20} meter re-aiming. Left: L_{20} FOV from typical observer, middle: L_{20} FOV from luminance meter aiming at portal centre, right: L_{20} FOV from luminance meter in an optimized aiming.

Under this concept, the new aiming point of the external L_{20} luminance meter should be appropriately selected in a way that the factors γ_m, ε_m, ρ_m and τ_m will be updated to γ_o, ε_o, ρ_o and τ_o to match the factors γ_n, ε_n, ρ_n and τ_n respectively. If an optimal solution is not possible, the priority of the optimisation procedure should be given to the factor with the highest corresponding luminance value (i.e. L_c, L_r, L_e), then to the factor with the next lower luminance where possible and so on.

Taking as an example a random L_{20} FOV where $L_c > L_r > L_e$, the FOV optimization procedure should be done in the following order:

First to optimize the sky percentage, i.e. $\gamma_o = \gamma_n$

then, if possible, to optimize road percentage, i.e. $\rho_o = \rho_n$

then, if possible, to optimize environment percentage, i.e. $\varepsilon_o = \varepsilon_n$

then, if possible, to optimize portal percentage, i.e. $\tau_o = \tau_n$

The re-aiming concept relies on the assumption that the reflectivity of the FOV components is considered almost Lambertian and thus the lateral position of the L_{20} meter does not affect the reflectivity of the materials. Thus, it is assumed that the luminance on a specific material (e.g. concrete surroundings) will have the same or almost the same luminance at the same time of the day measured from the driver's position and from the L_{20} meter position.

The analysis method and the results that are presented in the next section are developed in order to support and validate this re-aiming concept.

3 Analysis method and calculation parameters

The investigation of the effect of the variation of L_{20} and the effect on the energy consumption of a typical tunnel incorporates a vast amount of possible calculations. For this purpose, a special calculation algorithm was developed in order to handle thousands of calculations and to ensure that all possible cases were examined. The algorithm was developed using MATLAB software and was fed with data derived by the FOV compositions, daily daylight variations and level of installed power for the typical tunnel as described below.

3.1 Calculation method of potential FOVs

The L_{20} FOV comprises random percentages of sky, road, rocks, buildings, snow, and meadows. The composition of the FOV of the L_{20} meter versus the one of the FOV of the typical observer is critical. To determine how significant the mixture of elements in the FOV is, in terms of the total luminance, a parametric sensitivity analysis was realized. The scope of the analysis was to produce all the possible FOV combinations and to calculate the corresponding L_{20} luminance values in real tunnels. The reference luminance values for each component (sky, road, etc) were taken from CIE 88 in order to simulate the L_{20} calculation as it takes place in real practice.

For the simulation purposes, the four significant orientations of the tunnel portal were considered (North, East or West, and South) in accordance with the luminance values given in the CIE 88. In CIE 88, the sky is one of the components with the higher luminance values in all directions. Therefore, the sensitivity analysis that is presented in this paper was performed considering the variation of the sky percentage as the primary optimisation target. Furthermore, the other important component is the presence of snow. Since the presence or the absence of snow has a significant effect on the results, but snow is not considered as a potential component in all countries, there were two major simulation groups, one with consideration of snow and one without it.

In each set of calculations, the significant component was the percentage of the sky which ranged from 0 % up to 60 % in steps of 5 %. For each sky percentage value, all the possible combinations or FOV and therefore the L_{20} luminance amongst the other factors were calculated. The calculations were made using the equation (1) with the restriction of the equations (2) and (3). For the environment luminance L_e, the following 4 sub-components were considered according to CIE 88.

- L_{rock} = luminance of the rocks ζ = % of rocks in the 20° FOV
- L_{build} = luminance of the buildings η = % of buildings
- L_{snow} = luminance of the snow θ = % of snow
- L_{mead} = luminance of the meadows μ = % of meadows

The range of variation of each component of the FOV was taken as shown below. The limitations on the percentages were considered according to real situations.

- γ : from 0 % to 60% of the whole FOV in steps of 5 % (constant for each calculation set)
- ρ : from 20 % to 40 % of the whole FOV in steps of 1 %
- ε : from 15 % to 60 % of the whole FOV in steps of 1 %.
- ζ : from 0 % to 100 % of ε in steps of 1 %.
- η : from 0 % to 100 % of ε in steps of 1 %.
- θ : 0% when not considered or from 0 % to 100 % of ε in steps of 1 % when considered.
- μ : from 0 % to 100 % of ε in steps of 1 %

The above percentages should also follow equation (3). Therefore, any combination of the environment sub-components that does not sum 100 % is rejected.

$$\zeta + \eta + \theta + \mu = 1 \text{ or } 100\ \% \tag{3}$$

In the same concept, any of the combinations that do not sum 100 % of the L_{20} FOV are rejected from the calculations.

The final calculations of the L_{20} were made using equation (4)

$$L_{20} = \gamma\, L_c + \rho\, L_r + (\zeta\, L_{rock} + \eta\, L_{build} + \theta\, L_{snow} + \mu\, L_{mead})\, \varepsilon + L_{th}\, \tau \tag{4}$$

For the purpose of this investigation, L_{th} is considered negligible, compared to the other luminance values, and therefore is set equal to zero.

3.2 Calculation of the daylight variation

In order to examine the effect of the various L_{20} values on the total energy consumption of the tunnel, the daily variation of the exterior luminance (tunnel portal) is needed. For this reason, a daylight simulation was performed. The simulation is realized for the four significant orientations using the raytracing engine of the software Relux Desktop 2019. The location of the simulation was chosen to be one with an average Latitude coordinates in the middle of the northern hemisphere. The simulations were made for the 21st of March using CIE intermediate sky (CIE T6). This procedure exported the representative luminance variation $L_{rel}(t)$ for each orientation in a relative scale (0 to 1). The aim was to determine the average duration of the daylight and the relative variation of the luminance on a diffuse target facing at each one of the considered orientations. This relative luminance variation was fed in the calculation algorithm as it is explained below.

3.3 The typical tunnel under consideration

For the estimation of the energy consumption following the variation of the calculated L_{20}, a typical tunnel was considered. This typical tunnel has 2 traffic lanes of 3,75 m width on each lane and a total width of 10 m including the sidewalks. The height of the tunnel was selected to be 7 m. The length was selected equal to 700 m in order to accommodate the full length of the transition zone for speeds up to 120 kilometres per hour. A counter beam type luminaire was selected and was placed in a single central row at the middle of the tunnel at 6 m height. The efficacy of the luminaire (on several wattages) was set to 100 lm·W^{-1}. The design process was carried out using the dedicated software the Relux Tunnel (screenshots shown in Figure 2).

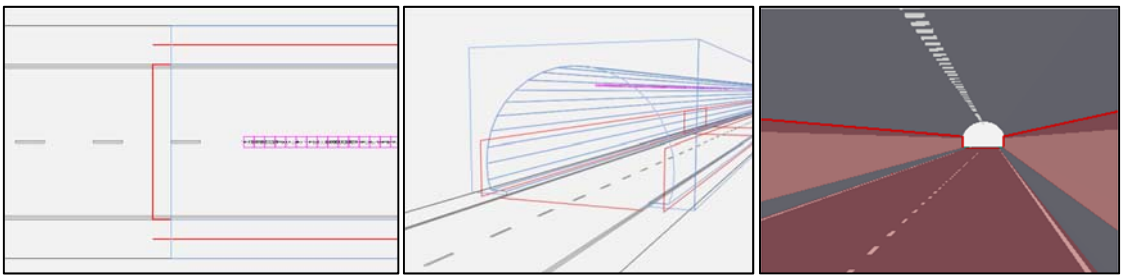

Figure 2 – Typical tunnel design using Relux Tunnel

Several calculations were made for various values of L_{th} and design speeds S varying from 80 km·h^{-1} to 120 km·h^{-1}. The total installed power of the reinforced lighting zone of the tunnel $P_t(L_{th}, S)$,was calculated for all the cases. The installed power of the interior zone was not considered as it is constant per kilometre while the reinforcement lighting is varying but independent of the tunnel length.

4 Calculation results

4.1 Analysis on the potential L_{20} FOVs

The developed calculation algorithm was fed with the data described in paragraph 3.1. The calculation results were grouped into 13 groups per orientation. In each one of the groups, the percentage of the sky was kept constant while the other components were varying as described in the previous paragraphs. The total number of calculations per group ranged from 150 000 to 350 000 depending on the possible FOV combinations. The results are presented in two ways using double figures. The first one is using histograms and the second is using the statistical box plot method.

Histograms have a colour code according to the corresponding sky percentage. All presented histograms have a bin width equal to 50 cd·m^{-2}. For the convenience of the reader, individual annotations were placed in the distributions assigned to 0 %, 35 % and 60 % of the sky. The box plots show the median value of the corresponding group of calculations with the red line. The borders of each box represent the 25 % and 75 % percentile while the outer calculated values are shown with vertical lines connected to the main box using dashed lines. Histograms reveal the distribution of each possible combination of the FOV (for a constant sky percentage)

and how each distribution overlaps with the next and previous one. On the other hand, the box plots illustrate the median of each distribution and the most significant range of values (25 % to 75 %) that are more probable to meet in real practice.

4.1.1 Analysis without considering the snow in the L_{20} FOV

The first set of calculations considers all the possible combinations of the L_{20} FOV without the presence of snow. Therefore, the percentage θ in equation (4) was always taken equal to zero. Figures 3 to 5 show the calculation results per direction of the tunnel portal.

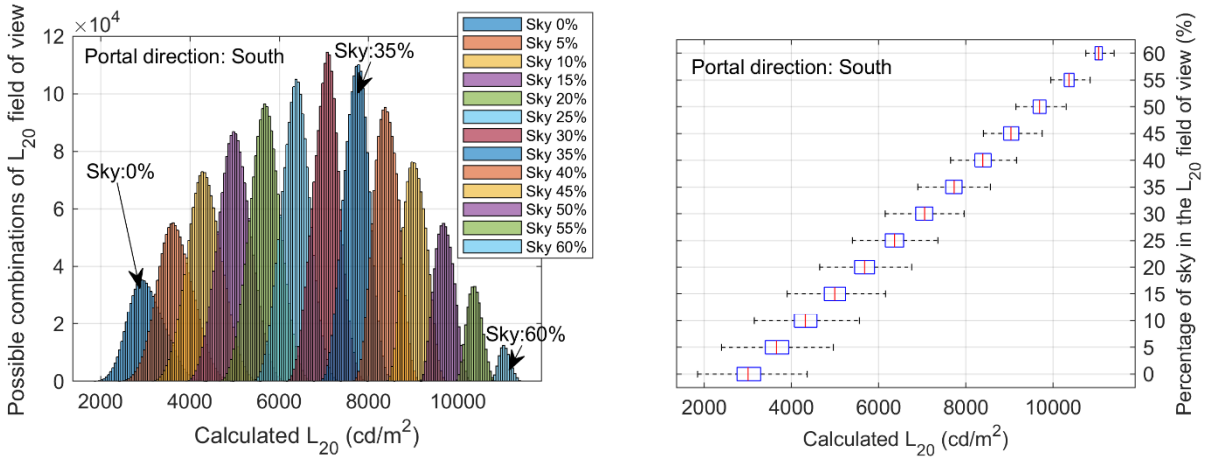

Figure 3 – Calculation results for Southern portal direction (no snow in FOV)

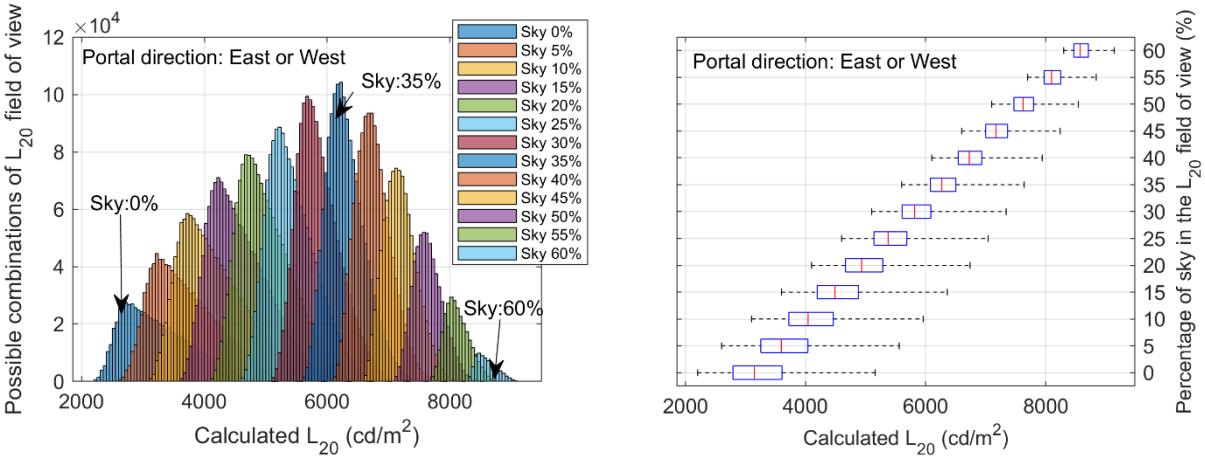

Figure 4 – Calculation results for Western or Eastern portal direction (no snow in FOV)

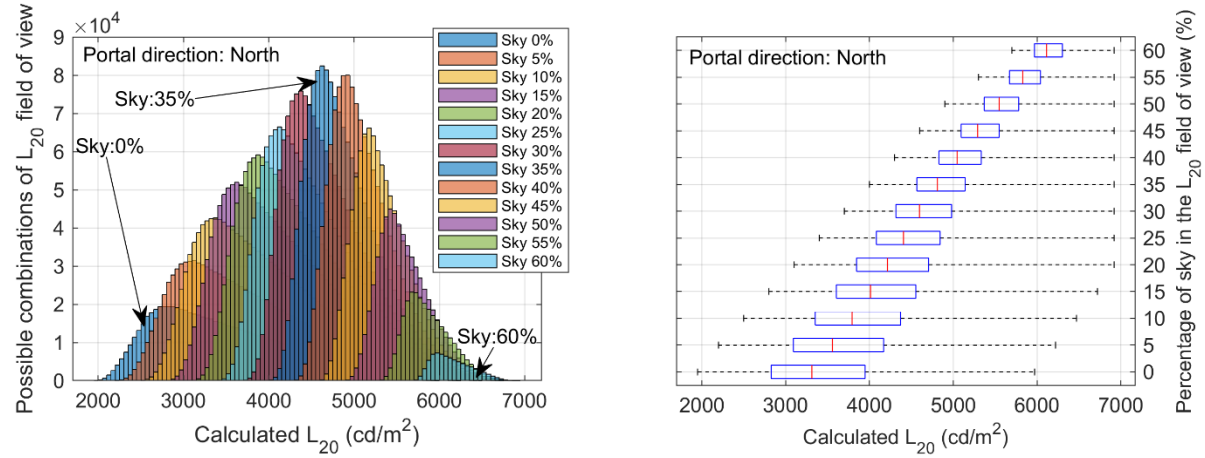

Figure 5 – Calculation results for Northern portal direction (no snow in FOV)

4.1.2 Analysis considering the snow in the L_{20} FOV

The second set of calculations considers all possible combinations of the L_{20} FOV with the presence of snow in the FOV. Therefore, the percentage θ in equation (4) varied in the same way as the remaining environment sub-components. Figures 6 to 8 show the calculation results per direction of the tunnel portal.

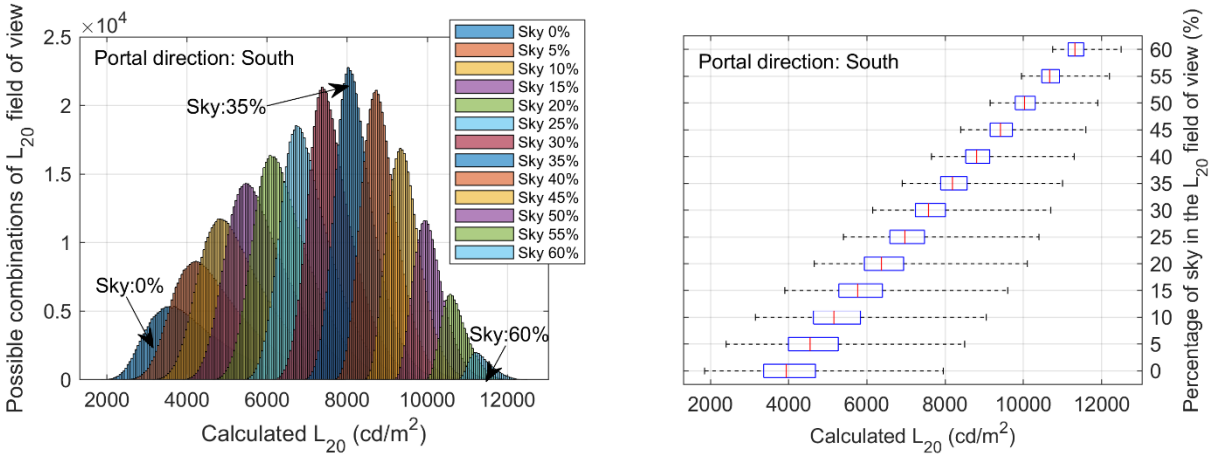

Figure 6 – Calculation results for Southern portal direction (snow in FOV)

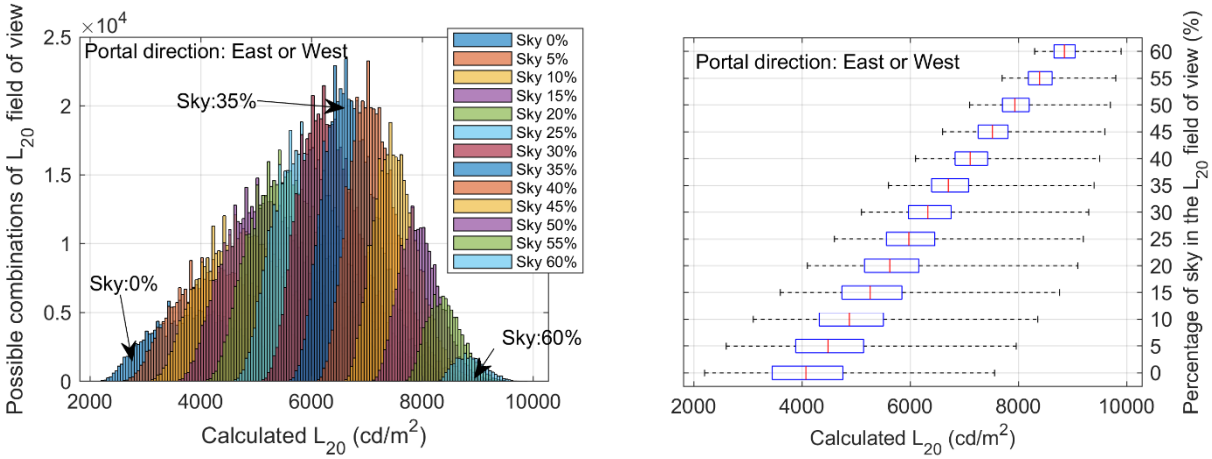

Figure 7 – Calculation results for Eastern or Western portal direction (snow in FOV)

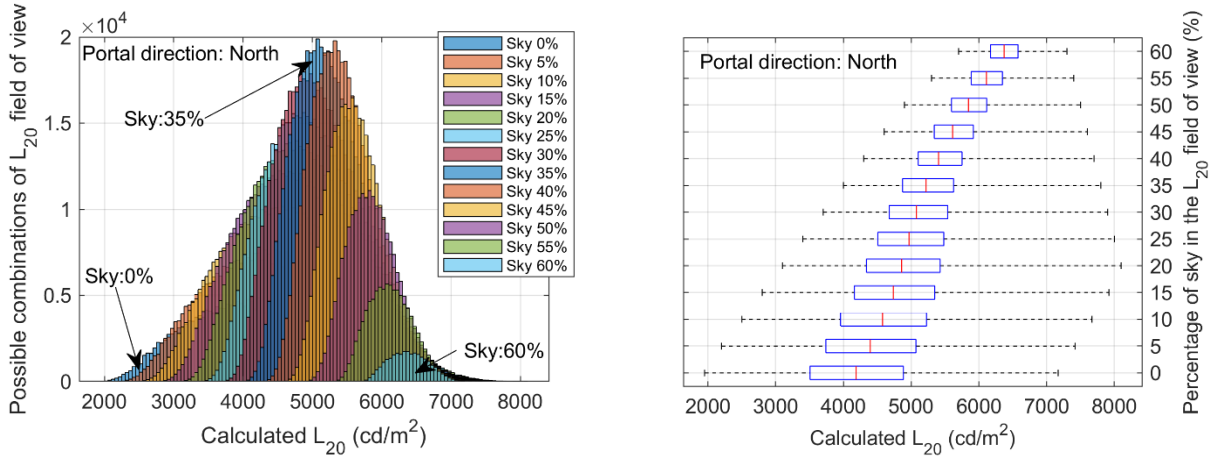

Figure 8 – Calculation results for Northern portal direction (snow in FOV)

4.2 Effect of L_{20} FOV on the annual energy consumption

The parametric analysis on the effect of the L_{20} FOV was concluded with the calculation of the expected effect on the annual energy consumption of the typical tunnel. Apart from the fact that the correct reading of the L_{20} meter ensures the correct triggering of the lighting control system and therefore increases the tunnel safety, an erroneous triggering of the luminaire groups will result in the increase or decrease of the energy consumption. Therefore, this analysis aims to provide some figures concerning this issue.

The calculation of the annual energy consumption can be made using the equation (5)

$$E_{\text{an}} = \int P_{\text{t}}(L_{\text{th}}, S)\, L_{\text{rel}}(t)\, \mathrm{d}t \tag{5}$$

where:

E_{an}: the annual energy consumption of the tunnel in kWh

$P_{\text{t}}(L_{\text{th}}, S)$: the power of the lighting system (in kW) for a given L_{th} and design speed S

$L_{\text{th}} = k\, L_{20}$: the luminance of the threshold zone

k: the ratio between L_{20} and L_{th} that depends on the design speed (acc. to CIE 88)

$L_{\text{rel}}(t)$: the relative variation of portal luminance along the day that depends on the orientation

For the purpose of this study, L_{th} was limited to 400 cd·m^{-2} independently of the calculated L_{20} and the factor k. This limitation was imposed as, in real practice, lighting systems in tunnels are designed to serve luminance levels not more than around 400 cd·m^{-2}. An extension of this limit can be therefore be considered if needed. If the calculated L_{th} was below 400 cd·m^{-2} then this specific level is considered in equation (5) for the corresponding annual energy calculation.

The calculation algorithm aimed to compare the possible difference in the energy consumption of all combinations between the nominal sky percentage (as seen by the typical observer) and the actual percentage of the sky in the FOV of the lateral luminance meter. Therefore, pairs of sky percentages were created, and the energy differences were calculated using equation (6).

$$\Delta E_{\text{an}} = (E_{\text{an, driver}} - E_{\text{an, meter}}) \cdot (E_{\text{an, driver}})^{-1} \cdot 100\ \% \tag{6}$$

where:

ΔE_{an} = the difference in annual energy consumption (%)

$E_{\text{an, driver}}$ = the annual energy consumption (nominal L_{20} as the triggering source)

$E_{\text{an, meter}}$ = the annual energy consumption (meter's L_{20} as the triggering source)

The $E_{\text{an, driver}}$ and the $E_{\text{an, meter}}$ are calculated using the equation (5) where the corresponding L_{20} is set equal to the one that is seen by the driver or the meter respectively. As the design of the lighting system is made considering the FOV of the typical driver, the L_{th} that is used in the energy calculations on equation (6) was set equal to the L_{th} as calculated for the driver's FOV and not over 400 cd·m^{-2} as described above. This is to ensure that the energy calculations consider the same installed power of the lighting system for each pair of sky percentages.

Tables 1 to 3 show the calculation results for the differences in energy consumption between all pairs of sky percentages and for the significant orientations and a design speed equal to 100 km·h^{-1}. All presented calculations are without the consideration of snow in the FOV. The remaining results (different design speeds and snow consideration) were skipped due to page limitation. ΔE_{an} was calculated based on the median value of L_{20} of the corresponding percentage of each pair of sky percentages. As mentioned above, these values are indicated with the red line in the box plots in Figures 3 to 5. This simulates the most likely or the most expected difference in annual energy consumption in the investigated cases.

As an example, in Table 1, when the sky percentage in the driver's L_{20} FOV is 15 % and the sky percentage in the meter's L_{20} FOV is 35 %, an increased energy consumption of around 27 % is expected due to the erroneous triggering of the control system.

Table 1 – Expected difference in the annual energy consumption for various sky percentages for Southern direction of the typical tunnel and design speed of 100km/h

ΔE_{an} (%)		Sky percentage in the FOV of the typical observer (%)												
		0	5	10	15	20	25	30	35	40	45	50	55	60
Sky percentage in the FOV of the meter (%)	0	0	-19	-32	-41	-47	-50	-52	-54	-55	-56	-56	-57	-58
	5	15	0	-16	-28	-35	-39	-41	-43	-45	-46	-46	-47	-48
	10	24	13	0	-14	-22	-27	-30	-32	-34	-35	-36	-37	-38
	15	31	21	12	0	-10	-15	-18	-21	-24	-25	-26	-27	-28
	20	35	27	19	10	0	-6	-10	-13	-16	-17	-18	-19	-21
	25	39	32	24	18	7	0	-4	-7	-10	-11	-13	-14	-15
	30	42	35	30	22	11	4	0	-3	-6	-8	-9	-11	-12
	35	46	38	33	27	15	8	4	0	-3	-5	-6	-8	-9
	40	50	41	35	31	18	11	7	3	0	-2	-3	-5	-6
	45	51	44	38	33	20	13	9	5	2	0	-2	-3	-5
	50	52	47	40	35	22	15	10	6	3	2	0	-2	-3
	55	54	49	43	37	24	16	12	8	5	3	2	0	-2
	60	55	51	45	39	26	18	14	10	7	5	3	2	0

Table 2 – Expected difference in the annual energy consumption for various sky percentages for Eastern or Western direction of the typical tunnel and design speed of 100km/h

ΔE_{an} (%)		Sky percentage in the FOV of the typical observer (%)												
		0	5	10	15	20	25	30	35	40	45	50	55	60
Sky percentage in the FOV of the meter (%)	0	0	-13	-23	-31	-37	-42	-45	-47	-49	-50	-51	-52	-53
	5	11	0	-12	-21	-28	-33	-37	-39	-41	-42	-44	-45	-46
	10	19	10	0	-10	-19	-24	-28	-31	-33	-35	-36	-38	-39
	15	23	17	9	0	-9	-15	-20	-23	-26	-27	-29	-31	-32
	20	28	21	15	8	0	-7	-12	-15	-18	-20	-22	-24	-25
	25	32	25	20	14	7	0	-5	-9	-12	-14	-16	-18	-19
	30	34	29	23	19	13	6	0	-4	-7	-9	-11	-13	-15
	35	36	32	27	22	18	10	4	0	-3	-5	-7	-10	-11
	40	39	34	31	25	21	14	7	3	0	-2	-5	-7	-8
	45	41	36	33	28	24	16	10	5	2	0	-2	-5	-6
	50	44	38	34	31	27	19	13	8	5	2	0	-2	-4
	55	46	40	36	33	30	22	15	11	7	5	2	0	-2
	60	49	43	38	35	32	24	17	13	9	7	4	2	0

Table 3 – Expected difference in the annual energy consumption for various sky percentages for Northern direction of the typical tunnel and design speed of 100km/h

ΔE_{an} (%)		Sky percentage in the FOV of the typical observer (%)												
		0	5	10	15	20	25	30	35	40	45	50	55	60
Sky percentage in the FOV of the meter (%)	0	0	-7	-13	-18	-22	-26	-29	-32	-35	-38	-40	-42	-43
	5	6	0	-6	-12	-16	-20	-23	-27	-30	-33	-35	-37	-39
	10	11	5	0	-6	-10	-14	-18	-22	-25	-28	-31	-33	-35
	15	15	10	4	0	-5	-9	-13	-17	-21	-24	-27	-29	-31
	20	18	13	9	4	0	-5	-9	-13	-17	-20	-23	-25	-27
	25	20	16	12	8	3	0	-4	-9	-13	-16	-19	-22	-24
	30	22	19	15	11	7	3	0	-5	-9	-12	-15	-18	-20
	35	24	21	18	14	11	7	4	0	-5	-8	-11	-14	-16
	40	26	23	20	17	14	11	8	4	0	-4	-7	-10	-12
	45	29	25	22	19	17	14	11	8	4	0	-4	-7	-9
	50	31	27	24	22	19	17	14	11	8	4	0	-3	-6
	55	33	30	27	24	22	20	17	14	11	7	3	0	-3
	60	34	32	29	26	24	22	20	18	14	10	6	3	0

5 Evaluation of the results and discussion

The result of the presented study shows a significant role of the L_{20} FOV in the calculation of both the L_{20} luminance and the corresponding energy consumption of the tunnel. The graphs presented in paragraph 3 show that the distribution of the possible L_{20} values is narrower and more separated in southern direction without snow in the FOV. Should the FOV involves the snow and the orientation changes towards East or South and North, the distribution of possible L_{20} values becomes wider with more overlaps. This finding reveals the importance of the correct luminance meter aiming especially in portals with Southern direction where a small change in the sky percentage is expected to result in a noticeable difference in L_{20} and E_{an}. The system becomes more elastic in other orientations were small differences are expected to have less impact in the energy consumption. Therefore, the re-aiming process can be done using the sky percentage as a primary optimisation target, while the remaining components should follow in the best possible way. The expected results will be among the calculated results shown in the corresponding graphs and tables. Further investigation should be done for all the intermediate orientations as well as taking into consideration the road, the buildings and the other components as the significant optimization FOV component.

References

BOUROUSSIS, C.A., TOPALIS, F.V. 2011. Energy saving in tunnel lighting by reducing the entrance luminance. Romanian Lighting Convention 2011 Conference, Bucharest, Romania

CIE 2004. CIE 88:2004. *Guide for the Lighting of Road Tunnels and Underpasses.* Vienna: CIE

CIE 2010. CIE 189:2010. *Calculation of Tunnel Lighting Quality Criteria.* Vienna: CIE

LORPHEVRE, R., DEROISY, B., DENEYER, A., DEHON, J. 2016. Method for Analysis of Annual Daylight Levels at Tunnel Approach. CIE 2016 Conference, Melbourne, Australia.

LOPEZ, J.C., GRINDLAY, A.L., PENA-GARCIA, A. 2017. A proposal for evaluation of energy consumption and sustainability of road tunnels: The sustainability vector. *Tunnelling and Underground Space Technology.,* 65, 53-61